



HAL
open science

Incorrect DFT-GGA predictions of the stability of non-stoichiometric/polar dielectric surfaces: The case of $\text{Cu}_2\text{O}(111)$

Niklas Nilius, Hanna Fedderwitz, Boris Gross, Claudine Noguera, Jacek Goniakowski

► **To cite this version:**

Niklas Nilius, Hanna Fedderwitz, Boris Gross, Claudine Noguera, Jacek Goniakowski. Incorrect DFT-GGA predictions of the stability of non-stoichiometric/polar dielectric surfaces: The case of $\text{Cu}_2\text{O}(111)$. *Physical Chemistry Chemical Physics*, 2016, 18, pp.6729-6733 10.1039/C5CP06933E . hal-01274702

HAL Id: hal-01274702

<https://hal.sorbonne-universite.fr/hal-01274702v1>

Submitted on 16 Feb 2016

HAL is a multi-disciplinary open access archive for the deposit and dissemination of scientific research documents, whether they are published or not. The documents may come from teaching and research institutions in France or abroad, or from public or private research centers.

L'archive ouverte pluridisciplinaire **HAL**, est destinée au dépôt et à la diffusion de documents scientifiques de niveau recherche, publiés ou non, émanant des établissements d'enseignement et de recherche français ou étrangers, des laboratoires publics ou privés.

Incorrect DFT- GGA predictions of the stability of non-stoichiometric/polar dielectric surfaces: The case of $\text{Cu}_2\text{O}(111)$

Niklas Nilius,^{1*} Hanna Fedderwitz,¹ Boris Groß,¹ Claudine Noguera,² Jacek Goniakowski^{2*}

¹ Carl von Ossietzky Universität Oldenburg, Institut für Physik, D-26111 Oldenburg, Germany

² CNRS-Sorbonne Universités, UPMC Univ. Paris 06, UMR 7588, INSP, F-75005 Paris, France

Corresponding Authors: nilius@fhi-berlin.mpg.de, jacek.goniakowski@insp.jussieu.fr.

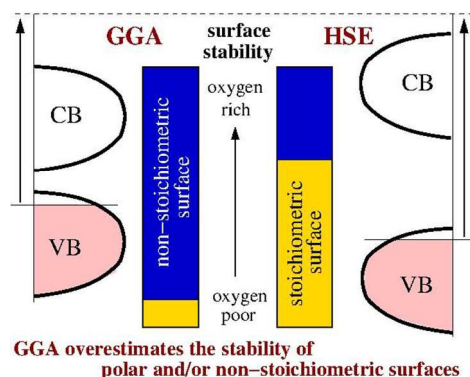
Abstract

Scanning tunneling microscopy (STM) and hybrid density functional theory (DFT) have been used to study the stability and electronic characteristics of the $\text{Cu}_2\text{O}(111)$ surface. We challenge previous interpretations of its structure and composition and show that only appropriate (hybrid) calculations can correctly account for the relative thermodynamic stability of stoichiometric versus Cu-deficient terminations. Our theoretical finding of the stoichiometric surface to be most stable at oxygen-lean conditions is confirmed by an excellent matching between STM spectroscopy data and the calculated surface electronic structure. Beyond the specific case of the $\text{Cu}_2\text{O}(111)$ surface, and beyond the known deficiencies of GGA-based approaches in the description of oxide electronic structures, our work highlights the risk of an erroneous evaluation of the surface stability, in cases where the energetics and electronic characteristics are strongly coupled, as in a wide class of polar and/or non-stoichiometric oxide surfaces.

Keywords

Hybrid exchange-correlation functional; ab initio thermodynamics; oxide surfaces and ultra-thin films; scanning tunneling microscopy and spectroscopy; cuprous oxide

TOC graphics



1 Introduction

A variety of outstanding properties make thin oxide films desirable materials for applications in optics, photovoltaics, microelectronics and heterogeneous catalysis.^{1,2,3} At small thickness, metal-supported oxide films can display a structural and stoichiometric flexibility not accessible to surfaces of bulk materials, which gives additional levers for tuning their properties.^{4,5,6} However, this complexity makes controlled fabrication and precise characterization of such objects particularly difficult and first-principles calculations have proven invaluable to interpret experimental data, such as complex scanning tunneling microscopy (STM) images.^{7,8}

The theoretical description of the physico-chemical properties of oxides often suffers from drawbacks of DFT-based *ab initio* methods using (semi-)local exchange-correlation functionals (LDA or GGA), which fail to correctly reproduce band-gaps and absolute positions of the band-edges.^{9,10} Although addition of an empirical Hubbard term (GGA+U) partially corrects the problem in cases where transition metal atoms are involved,¹¹ this approach turns out to be inefficient for compounds with simple *sp* atoms or closed cationic *d* (or *f*) shells.^{12,13,14} While deficiencies in the description of oxide electronic properties by GGA-based methods have been discussed in numerous studies, much less is known on their impact on the surface thermodynamics. Relying on the particularly striking example of the Cu₂O(111) surface, we will show that the problem principally concerns polar/non-stoichiometric surfaces, and may lead to an erroneous estimation of their stability.

The (1×1)-Cu₂O(111) surface has been systematically explored on bulk samples^{15,16} and ultra-thin metal-supported films.^{17,18} Since the hexagonal pattern observed in STM images exhibits symmetry and spacing of both coordinately unsaturated Cu and O atoms (Cu_{CUS} and O_{CUS}), models based on either a non-polar stoichiometric (Cu_{CUS} and O_{CUS} present at the surface) or a polar Cu-deficient termination (only O_{CUS} present) have been proposed.^{19,20} These two terminations were indeed shown to be by far the most stable and the existing GGA and GGA+U calculations predict that the Cu-deficient termination is favored over the entire range of relevant oxygen chemical potentials,^{19,21,22} suggesting that reactive Cu_{CUS} species are absent at the surface and that the outermost O_{CUS} are responsible for the observed STM contrast.

The goal of the present work is two-fold. First, on the basis of STM measurements combined with hybrid DFT calculations, we challenge the existing interpretation of the (1×1)-Cu₂O(111) surface.^{19,21,21,23} We find that, at this approximation level of the exchange-correlation functional, the stoichiometric termination is more stable than the Cu-deficient one at oxygen-lean conditions. More generally, and beyond the particular (1×1)-Cu₂O(111) system, we highlight the sensitivity of the surface thermodynamics to the level of description of the electronic structure and show that, in addition to giving inaccurate electronic properties, (semi-)local DFT approaches may lead to erroneous predictions of surface stability. General arguments show that this may occur in a wide class of polar/non-stoichiometric oxide surfaces with a non-insulating ground state.

2 Experimental and computational methods

The experiments have been performed in a custom-built ultra-high vacuum STM, operated at liquid-nitrogen temperature. Cuprous oxide films were prepared by Cu deposition (0.25 ML/min) onto a sputtered and annealed Au(111) single crystal in an O₂ ambience of 5×10^{-6} mbar at room temperature.¹⁸ After deposition, the samples were gently annealed to 600 K at $p < 10^{-9}$ mbar to promote ordering. The nominal oxide thickness was adjusted to 2-3 Cu₂O trilayers. Thicker films could not be stabilized, as layers of Cu metal started to form at the Au-oxide interface. STM imaging and conductance spectroscopy were carried out in the constant current mode and with a lock-in technique, respectively.

Calculations have been performed within the DFT framework implemented in VASP.²⁴ Beyond standard GGA (PW91),²⁵ the hybrid (HSE06)²⁶ approximation to the exchange-correlation functional has been used as to improve the description of the Cu₂O band gap E_g . The calculated HSE gap width (1.96 eV) increases significantly over the GGA (0.4 eV) and is close to the experimental value of 2.15 eV.²⁷ Let us note that the HSE gap is also much larger than those obtained within GGA+U approximation (0.5-0.8 eV, for U = 2-8 eV, respectively).¹⁴ While HSE significantly improves the calculated electronic structure, it impacts only little the bulk and surface structural characteristics. We find the bulk Cu₂O lattice parameter of 4.31 Å and 4.29 Å in HSE and GGA, respectively, compared to the experimental value of 4.27 Å. At the stoichiometric (111) surface, both approximations consistently predict a 2% reduction and a 3% expansion of the Cu-O_{CUS} and Cu_{CUS}-O bond lengths, respectively. The interaction of valence electrons with ionic cores is described within the projector augmented wave method.²⁸ Standard copper and gold, and soft oxygen (energy cutoff of 270 eV) pseudopotentials provided by VASP were used, enabling a complete structural relaxation at the hybrid level for all considered systems. GGA results obtained with the soft and the full (energy cutoff of 400 eV) oxygen pseudopotential were confronted and showed very satisfactory agreement (difference of bulk Cu₂O lattice parameter smaller than 0.01 Å, difference of (1x1) surface energies below 0.002 eV/Å²).

Bulk-cut Cu₂O(111) surface can be seen as a stacking of O-4Cu-O trilayers. In the direction perpendicular to the surface the subsequent Cu planes are fcc-stacked and distant by 2.5 Å. Oxygen layers are positioned at 0.6 Å above and below each of Cu planes, such that each oxygen atom forms three O-Cu bonds with the copper atoms from the Cu plane within the trilayer and a single bond with a Cu atom from the neighboring trilayer. Ultra-thin Au-supported films are modeled by slabs composed of three such O-4Cu-O trilayers in contact with a three-layer Au(111) film. A (1×1)-Cu₂O(111) // (2×2)-Au(111) unit cell with the in-plane lattice parameter of bulk Au is used. Thick unsupported Cu₂O(111) films are modeled with symmetric slabs composed of six O-4Cu-O trilayers at the calculated in-plane lattice parameter of bulk Cu₂O (6.10/6.07 Å in GGA/HSE, respectively). In all calculations, slabs are separated by at least 10 Å of vacuum and dipole correction is applied to slabs with two non-equivalent terminations. The Brillouin zone of the surface unit cell is sampled with a (4×4×1) Monkhorst-Pack k-point grid.²⁹ Atomic coordinates

of all ions in the oxide film are relaxed until residual forces dropped below 0.01 eV/Å, while the in-plane coordinates of the Au atoms are kept fixed. Film formation energies as a function of oxygen chemical potential $\Delta\mu_{\text{O}}$ were estimated with usual ab-initio thermodynamics expression:³⁰

$$\Gamma(\Delta\mu_{\text{O}}) = (E_{\text{film+substrate}} - E_{\text{bulk}} - E_{\text{substrate}} - n_{\text{O}}(\Delta\mu_{\text{O}} + E_{\text{O}_2}/2))/S$$

Here, $E_{\text{film+substrate}}$, E_{bulk} , $E_{\text{substrate}}$, and E_{O_2} are the calculated total energies of the supported oxide film, bulk Cu_2O for the same number of formula units, bare Au support, and free O_2 molecule, respectively. S is the area of the surface unit cell, while n_{O} represents the oxygen excess in the film with respect to bulk Cu_2O stoichiometry. For unsupported films, the substrate-related energy terms have been omitted.

3 Results

The oxide films have been prepared under extremely oxygen-lean conditions, close to the limit of Cu_2O stability, as witnessed by the formation of small metallic Cu clusters on the surface. The oxide chemical composition has been determined to be close to Cu_2O , employing core level and Auger spectroscopy.¹⁸ According to STM measurements, the films homogeneously wet the Au(111) surface and form large terraces delimited by the initial step edges of the support (Fig. 1a). Closer inspection reveals a hexagonal atomic pattern with ~ 5.9 Å periodicity, arranged in elongated domains of ~ 200 Å length and 25-35 Å width (Fig. 1b,c). These patterns coincide with the symmetry and spacing of either coordinatively unsaturated Cu_{CUS} or O_{CUS} sites on (1×1)- Cu_2O (111) surface (Fig. 2a). While both sites coexist on the stoichiometric (1×1) termination, only O_{CUS} is present at the Cu-deficient (1×1)- Cu_{CUS} surface. However, neither the termination of the oxide film nor the origin of the observed contrast can be assessed by STM alone. The electronic properties of the Cu_2O films are characterized by a band gap of ~ 1.8 eV, as derived from STM conductance spectra (Fig. 1d). The value is smaller than the reported bulk gap of Cu_2O (2.15 eV), reflecting the limited film thickness.²⁷ A pronounced surface state is visible at 0.9 V in the unoccupied, upper half of the band gap. In contrast to the oxide ad-layer, the pristine gold exhibits a step-like conductance onset at -0.5 V, a feature that is readily assigned to the Shockley surface states residing on Au(111).³¹

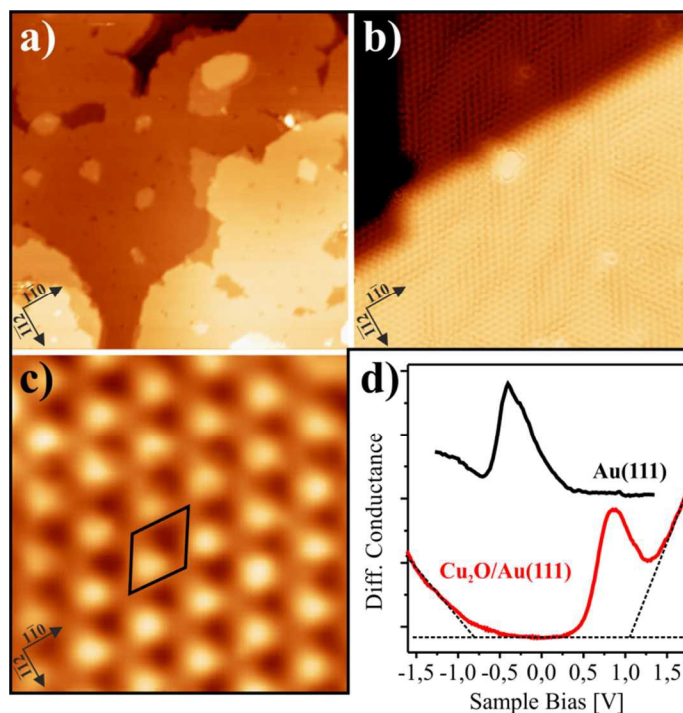


Fig. 1: (a-c) Overview ($100 \times 100 \text{ nm}^2$), medium-sized ($25 \times 25 \text{ nm}^2$), and atomically resolved with indication of the (1×1) unit-cell ($3.3 \times 3.3 \text{ nm}^2$) STM images of Cu_2O films grown on Au(111) ($U_s = 0.8 \text{ V}$, 0.1 nA). (d) STM conductance spectra of bare Au(111) (black) and Cu_2O ad-layers (red). Band-edge slopes for determination of the gap size are shown as dashed lines. Note the surface state at 0.9 V in the oxide spectrum.

To analyze the experimental results, we have modeled a three-trilayer thick (1×1) - $\text{Cu}_2\text{O}(111)$ film on Au(111) by DFT calculations. We find that the gold substrate stabilizes the Cu_{CUS} and destabilizes the O_{CUS} at the film termination in contact with the metal. This produces an overall copper excess in the film and leads to a non-equivalence of its interface and surface structure. At the film surface, the (1×1) and (1×1) - Cu_{CUS} terminations compete. GGA calculations predict the Cu_{CUS} -deficient surface to be the most stable over the entire range of relevant oxygen chemical potentials (Fig 2b). The stoichiometric (1×1) termination is found to be stable only at $\Delta\mu_{\text{O}} < -2.4 \text{ eV}$, thus far beyond the calculated bulk Cu_2O stability limit of -1.37 eV . Note that correction for the known over-binding of the O_2 molecule in GGA shifts the $\Delta\mu_{\text{O}}$ scale by roughly -0.45 eV , making the calculated Cu_2O stability limit consistent with the experimental Cu_2O formation energy of -1.75 eV .³² This does however not alter the thermodynamic instability of the (1×1) termination predicted by GGA.

Conversely, the hybrid HSE approach finds the stoichiometric surface to be favored at realistic oxygen-lean conditions, $\Delta\mu_{\text{O}} < -1.7 \text{ eV}$. The latter are close to, but still above the HSE stability limit of bulk Cu_2O of -1.83 eV . The difference between GGA and HSE predictions is therefore of qualitative nature. According to GGA, the stoichiometric (1×1) termination cannot be realized within the Cu_2O stability range, while HSE predicts such a possibility at highly oxygen-lean

conditions. The occurrence of such extreme conditions in the actual experiments is compatible with the observed formation of metallic Cu clusters on the oxide film.

Electronically, the stoichiometric (1×1) termination remains insulating with the Fermi level within the band gap (Fig. 2c). It develops an empty surface state of mixed $\text{Cu}_{\text{CUS}} s - \text{O}_{\text{CUS}} p_{x,y}$ character below the bottom of the conduction band, in good agreement with the gap state observed experimentally (Fig. 1d). The energy position is governed by the reduced electrostatic potential at the coordinately unsaturated surface ions; the calculated accuracy is limited by well-recognized problems of handling metallic substrates with hybrid functionals. At the (1×1)- Cu_{CUS} termination, at variance, the top of the oxide valence band is depleted (Fig. 2c) due to holes left by the missing neutral Cu_{CUS} . This leads to a metallization of the surface and to the formation of what is often referred to as a two-dimensional hole-gas (2DHG). The depletion can also be seen as positive compensating charge-density required for the electrostatic stabilization of the (1×1)- Cu_{CUS} termination, which is a polar type-2 surface according to Tasker's classification.^{33,34} Note that the surface-metallic nature of the (1×1)- Cu_{CUS} termination is inconsistent with the conductance spectra that unambiguously reveal a band gap around the Fermi level (Fig. 1d).

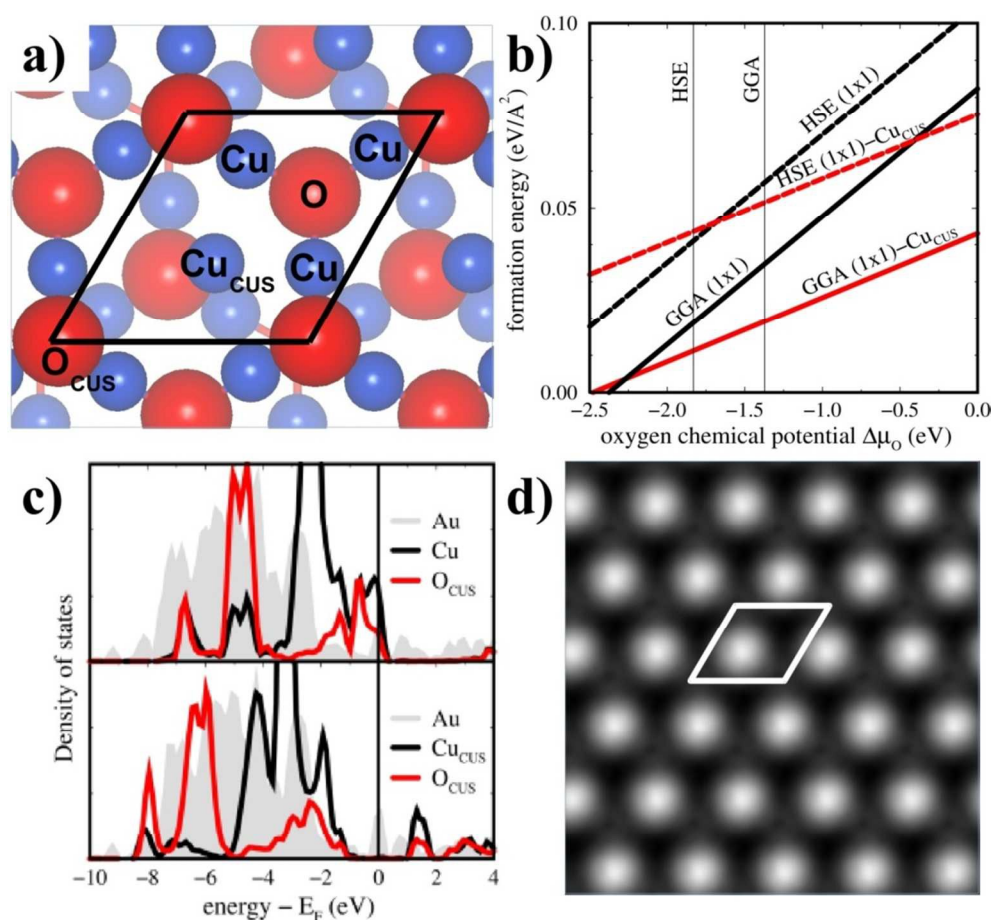


Fig. 2: Au(111)-supported (1×1)- Cu_2O (111) films. (a) Ball and stick model of the stoichiometric termination; Cu_{CUS} ions are missing at the Cu-deficient (1×1)- Cu_{CUS} surface. (b) GGA and HSE film formation energies with respect to bulk cuprous oxide as a function of the oxygen chemical potential $\Delta\mu_{\text{O}}$. Calculat-

ed limits of bulk Cu₂O stability are indicated by vertical lines. (c) HSE surface DOS of the Cu-deficient (top) and stoichiometric (bottom) terminations. (d) Simulated STM image at 2 V sample bias of the stoichiometric termination.

To elucidate the origin of the STM contrast produced by the empty gap state in the stoichiometric termination, we have employed the Tersoff-Hamman model to simulate STM images.³⁵ At a positive bias large enough to sample the surface state (above 0.8 and 1.5 eV in experiment and HSE, respectively), the bright spots correspond to the Cu_{CUS} ions despite the mixed Cu_{CUS}-O_{CUS} character of the state (Fig. 2d). Apparently, the purely geometric effect (O_{CUS} located nearly 1 Å more outwards than Cu_{CUS}) is overridden by an electronic contribution, induced by the diffuse character of Cu_{CUS} *s* orbital compared to the directional O_{CUS} *p_{x,y}* orbitals. Thus, our experimental and computational results show converging evidences that the stoichiometric Cu₂O(111) and not the Cu-deficient termination is obtained at the vacuum annealing conditions employed in our UHV experiment. They also prove that hybrid calculations are qualitatively superior in predicting the relative stability of the two terminations.

4 Discussion

Beyond comparing theory and experiment in the particular case of ultra-thin supported Cu₂O(111) films, we now wish to analyze the discrepancy between the two computational approaches and to link it to a peculiarity of the surface electronic structure. For this purpose, we have simulated thick unsupported Cu₂O(111) films, composed of six O-4Cu-O trilayers, representative for a bulk oxide termination. In agreement with previous results,^{19,21} our GGA calculations show that the Cu-deficient (1×1)-Cu_{CUS} is favored over the stoichiometric (1×1) surface in the entire stability range of bulk Cu₂O (Fig. 3a). HSE calculations, on the other hand, produce a qualitatively different stability picture, in which the stoichiometric (1×1) termination is favored over a relatively large span of oxygen-lean conditions under which bulk Cu₂O is thermodynamically stable (-1.83 eV < Δμ_O < -1.4 eV). The pronounced difference between GGA and HSE results goes beyond the effect of an improved binding of the O₂ molecule in HSE.³⁶ It is rather to be linked to the Cu-deficient, hence polar character of the (1×1)-Cu_{CUS} termination, which induces surface metallicity (Fig. 3b). This makes its energetics particularly sensitive to the quality of description of its electronic structure, whereas the energy of the insulating, stoichiometric surface depends much less on the level of approximation (Fig. 3a).

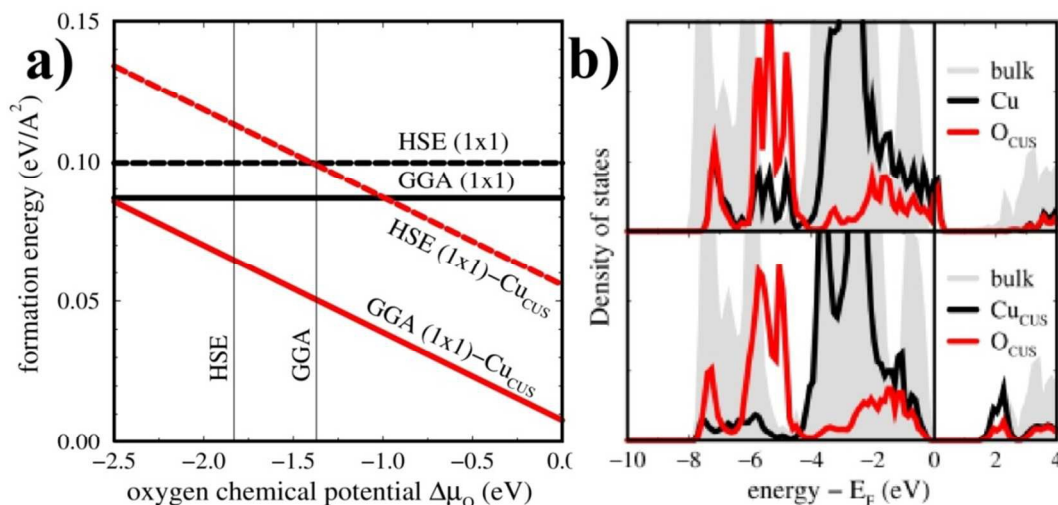


Fig. 3: Thick unsupported (1×1)-Cu₂O(111) films. (a) GGA and HSE formation energies with respect to the bulk oxide as a function of oxygen chemical potential $\Delta\mu_{\text{O}}$. Calculated limits of bulk Cu₂O stability are indicated by vertical lines. (b) HSE surface DOS for Cu-deficient (top) and stoichiometric (bottom) terminations.

The substantial energy difference from one level of approximation to another is thus mainly assigned to the cost of metallization of the surface, i.e. to the creation of holes at the top of valence band (present case) or electrons at the bottom of conduction band (oxygen-poor terminations). It is related to the surface ionization potential or electron affinity, which are more correctly described in HSE than in GGA. In the particular case of Cu₂O(111), the HSE ionization potential is 0.8 eV larger than the GGA estimation, given the substantial downward shift of the valence band. A similar effect is expected for many other oxide surfaces, whenever the electronic structure is non-insulating. In these cases, GGA predictions may systematically overestimate their stability with respect to insulating configurations. An additional energy contribution is present for extracting neutral atoms from non-stoichiometric, metallic surface, for which the improved HSE ionization potentials and electron affinities may be important as well.

5 Conclusion

By means of STM experiments and hybrid DFT calculations, we have studied the structural and electronic properties of (1×1)-Cu₂O(111) films grown on an Au(111) support. Besides a well-reproduced oxide band gap, we have shown that the improved description of the surface energetics with hybrid calculations increases the thermodynamic stability of the stoichiometric with respect to the Cu-deficient surface at oxygen-lean conditions, contradicting previous GGA-based studies. This finding is confirmed by the good agreement between experimental conductance spectra and the calculated DOS for this termination.

Beyond clarifying a controversy on the nature of the thermodynamically favored (1×1)-Cu₂O(111) surface, our results highlight the sensitivity of the energetics of non-insulating terminations to the level of description of their electronic structure. It is clear that, apart from the specific Cu₂O case, a correct estimation of the energy cost for surface metallization, induced either

by surface polarity or non-stoichiometry, requires a reliable description of the electronic structure.

Acknowledgements

This work has been supported by the COST Action CM1104 *Reducible oxide chemistry, structure and functions*, as well as by the DFG grant *Exploring photocatalytic processes at atomic scales*. N.N. thanks the graduate school 'Nanoenergy' for financial support. J. G. and C. N. gratefully acknowledge the generous allocation of computing time at IDRIS under project no. 100170.

References

- ¹ Q. Fu, T. Wagner, *Surf. Sci. Rep.*, 2007, **62**, 431-498.
- ² N. Nilius and H.-J. Freund, *Acc. Chem. Res.*, 2015, **48**, 1532.
- ³ L. Giordano and G. Pacchioni, *Acc. Chem. Res.*, 2011, **44**, 1244.
- ⁴ H. Kuhlenbeck, S. Shaikhutdinov and H.-J. Freund, *Chem. Rev.*, 2013, **113**, 3986.
- ⁵ C. Noguera and J. Goniakowski, *Chem. Rev.*, 2013, **113**, 4073.
- ⁶ S. Surnev, A. Fortunelli and F. P. Netzer, *Chem. Rev.*, 2013, **113**, 4314.
- ⁷ G. Kresse, M. Schmid, E. Napetschnig, M. Shishkin, L. Köhler, and P. Varga, *Science*, 2005, **308**, 1440.
- ⁸ L. Giordano, G. Pacchioni, J. Goniakowski, N. Nilius, E. D. L. Rienks, and H.-J. Freund, *Phys. Rev. B*, 2007, **76**, 075416.
- ⁹ J. P. Perdew and M. Levy, *Phys. Rev. Lett.*, 1983, **51**, 1884.
- ¹⁰ L. J. Sham and M. Schlüter, *Phys. Rev. Lett.*, 1983, **51**, 1888.
- ¹¹ V. I. Anisimov, J. Zaanen and O. K. Andersen, *Phys. Rev. B*, 1991, **44**, 943.
- ¹² A. Janotti and C. G. Van de Walle, *Phys. Rev. B*, 2007, **76**, 165202.
- ¹³ A. K. Singh, A. Janotti, M. Scheffler and C. G. Van de Walle, *Phys. Rev. Lett.*, 2008, **101**, 055502.
- ¹⁴ L. Y. Isseroff and E. A. Carter, *Phys. Rev. B*, 2012, **85**, 1.
- ¹⁵ K. H. Schulz and D. F. Cox, *Phys. Rev. B*, 1991, **43**, 1610.
- ¹⁶ A. Önstén, M. Göthelid and U. O. Karlsson, *Surf. Sci.*, 2009, **603**, 257.
- ¹⁷ F. Jensen, F. Besenbacher and I. Stensgaard, *Surf. Sci.*, 1992, **269-270**, 400.
- ¹⁸ H. Sträter, H. Fedderwitz, B. Groß and N. Nilius, *J. Phys. Chem. C*, 2015, **119**, 5975.
- ¹⁹ A. Soon, M. Todorova, B. Delley and C. Stampfl, *Phys. Rev. B*, 2007, **76**, 129902E.
- ²⁰ C. Li, F. Wang, S. F. Li, Q. Sun and Y. Jia, *Phys. Lett. A*, 2010, **374**, 2994.
- ²¹ L. Isseroff Bendavid and E. A. Carter, *J. Phys. Chem. B*, 2013, **117**, 15750.
- ²² A. Soon, M. Todorova, B. Delley and C. Stampfl, *Surf. Sci.*, 2007, **601**, 5809.
- ²³ M. M. Islam, B. Diwara, V. Maurice and P. Marcus, *Surf. Sci.*, 2009, **603**, 2087.
- ²⁴ G. Kresse and J. Hafner, *Phys. Rev. B*, 1994, **49**, 14251; G. Kresse and J. Furthmüller, *Phys. Rev. B*, 1996, **54**, 11169.
- ²⁵ J. P. Perdew, J. A. Chevary, S. H. Vosko, K. A. Jackson, M. R. Pederson, D. J. Singh and C. Fiolhais, *Phys. Rev. B*, 1992, **46**, 6671.
- ²⁶ J. Heyd, G. E. Scuseria and M. Ernzerhof, *J. Chem. Phys.*, 2003, **118**, 8207.
- ²⁷ B. K. Meyer, A. Polity, D. Reppin, M. Becker, P. Hering, P. J. Klar, T. Sander, C. Reindl, J. Benz, M. Eickhoff, C. Heiliger, M. Heinemann, J. Blasing, A. Krost, S. Shokovets, C. Müller and S. Ronning, *Phys. Status Solidi B*, 2012, **249**, 1487.
- ²⁸ G. Kresse and D. Joubert, *Phys. Rev. B*, 1999, **59**, 1758.

-
- ²⁹ H. Monkhorst and J. Pack, *Phys. Rev. B*, 1976, **13**, 5188.
- ³⁰ K. Reuter and M. Scheffler, *Phys. Rev. B*, 2001, **65**, 035406.
- ³¹ Y. Hasegawa and Ph. Avouris, *Phys. Rev. Lett.*, 1993, **71**, 1071.
- ³² M. W. Chase Jr., *NIST-JANAF thermochemical tables. American Institute of Physics for the National Institute of Standards and Technology*, American Chemical Society Washington, DC, New York 1998.
- ³³ P. W. Tasker, *J. Phys. C*, 1979, **12**, 4977.
- ³⁴ J. Goniakowski, F. Finocchi and C. Noguera, *Rep. Prog. Phys.*, 2008, **71**, 016501.
- ³⁵ J. Tersoff and D. R. Hamann, *Phys. Rev. Lett.*, 1983, **50**, 1998.
- ³⁶ S. Prada, L. Giordano, G. Pacchioni, C. Noguera and J. Goniakowski, *J. Chem. Phys.*, 2014, **141**, 144702.